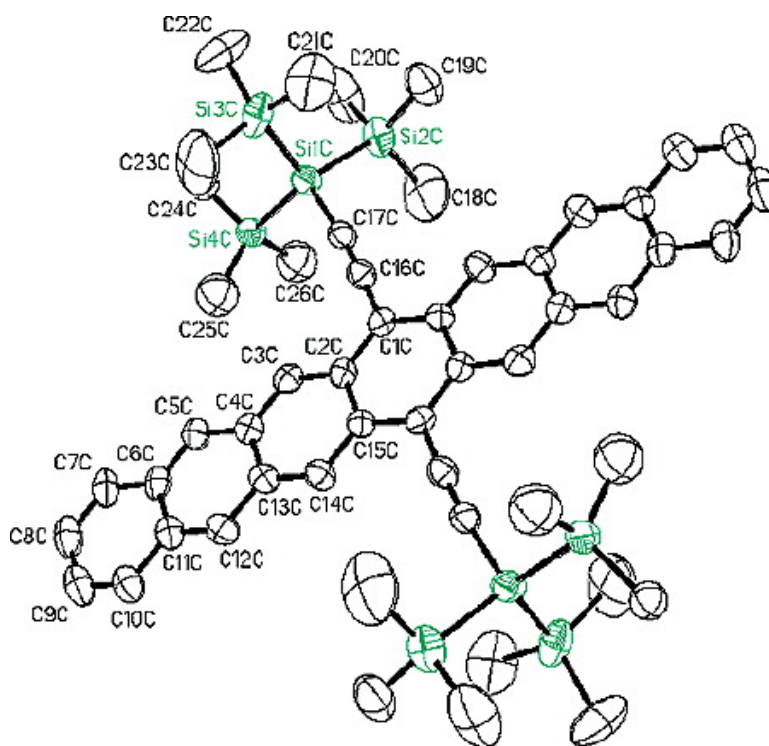


## Functionalized Higher Acenes: Hexacene and Heptacene

Marcia M. Payne, Sean R. Parkin, and John E. Anthony

*J. Am. Chem. Soc.*, **2005**, 127 (22), 8028-8029 • DOI: 10.1021/ja051798v • Publication Date (Web): 14 May 2005

Downloaded from <http://pubs.acs.org> on March 25, 2009



### More About This Article

Additional resources and features associated with this article are available within the HTML version:

- Supporting Information
- Links to the 31 articles that cite this article, as of the time of this article download
- Access to high resolution figures
- Links to articles and content related to this article
- Copyright permission to reproduce figures and/or text from this article

[View the Full Text HTML](#)



**ACS Publications**  
 High quality. High impact.

## Functionalized Higher Acenes: Hexacene and Heptacene

Marcia M. Payne, Sean R. Parkin, and John E. Anthony\*

Department of Chemistry, University of Kentucky, Lexington, Kentucky 40506-0055

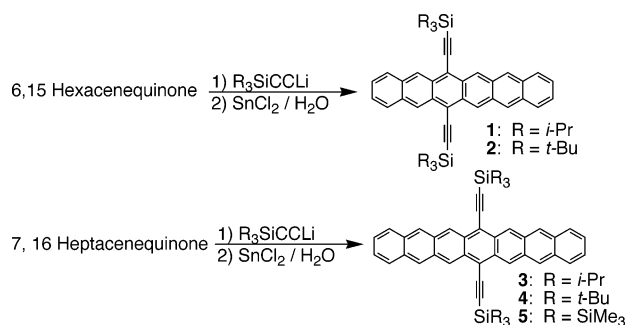
Received March 21, 2005; E-mail: anthony@uky.edu

The electronic properties of pentacene are exceptionally well-known, making it a common benchmark in the field of organic electronics.<sup>1</sup> Higher acenes, however, remain virtually unknown. Hexacene has received some crystallographic attention and appears in the solid state to follow a homologous series with tetracene and pentacene; however, there was insufficient data to actually solve and refine the structure.<sup>2</sup> Its low stability, combined with poor solubility, has made its preparation and study difficult.<sup>3</sup> Heptacene is even less well understood. Of the few reported syntheses, all have been called into question.<sup>4</sup> The only characterization data reported to date are a combustion analysis<sup>5</sup> and a UV-vis spectrum with estimated NIR bands.<sup>6</sup> While fullerene adducts of heptacene<sup>7</sup> and several examples of benzannulated heptacene have been reported,<sup>8</sup> none of these derivatives exhibit the unique electronic properties expected of the heptacene chromophore. Theoretical treatments of the acene family over the last several decades predict an array of properties for the higher acenes,<sup>9</sup> and controversy still exists over whether acenes as small as heptacene even possess a closed-shell ground state.<sup>10</sup>

Our work on soluble functionalized pentacene has shown that, in addition to providing increased solubility and improved crystalline order for device applications, the silylethynylation of acenes led to an increase in stability,<sup>11</sup> leading us to believe that this strategy might yield improved stability and solubility for higher acenes. We report here the application of our silylethynylation methods to the synthesis and characterization of hexacene and heptacene derivatives.

We followed the same two-step sequence to prepare functionalized higher acenes that was used for substituted pentacenes (Scheme 1).<sup>11a</sup> Our recent work with 7-ringed acenedithiophenes

### Scheme 1



demonstrated that the TIPS group, although often used as a protecting group for alkynes in Diels-Alder reactions,<sup>12</sup> is not sufficiently bulky to prevent Diels-Alder addition of the alkyne across reactive longer acenes.<sup>13</sup> This level of reactivity was also clearly an issue with the carbocyclic acenes, as neither of the TIPS-substituted higher acenes (**1**, **3**) were stable in solution or in the solid state. As with the acenedithiophenes, use of the bulkier alkyne tri-*tert*-butylsilyl (TTBS) acetylene led to a dramatic increase in stability. Chromatographic purification of the deep-green solution

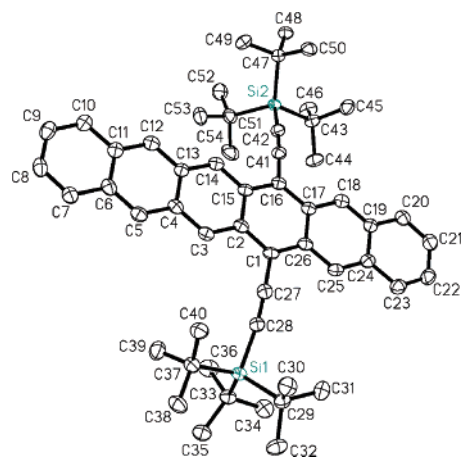
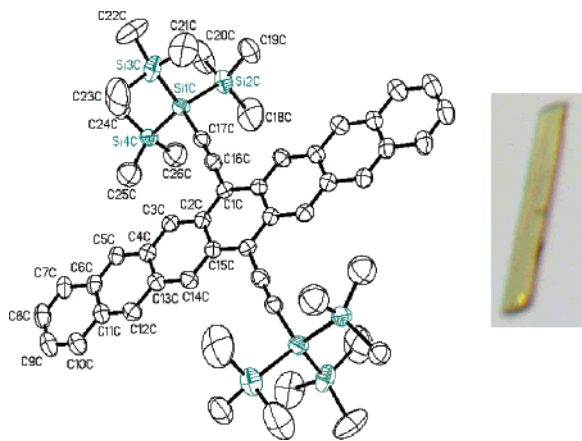


Figure 1. X-ray crystal structure of **2**.

of hexacene **2** followed by recrystallization led to faceted green blocks well suited to study by single-crystal X-ray diffraction (Figure 1). Although a small amount (9%) of disorder is apparent in the hexacene backbone,<sup>14</sup> analysis of the crystalline order of **2** revealed a two-dimensional  $\pi$ -stacked arrangement similar to that of pentacene derivatives exhibiting high hole mobility.<sup>15</sup> While the aromatic backbone of **2** is planar to within 0.1 Å, the alkynes are bent dramatically, presumably to alleviate the strains of crystal packing. Hexacene **2** is quite soluble, allowing full spectroscopic characterization. Cyclic voltammetry revealed one reversible oxidation at 0.660 V vs SCE and a reversible reduction at -0.925 V vs SCE. The low reduction potential is in part due to the presence of the silicon functional group, a factor that has been implicated in the increased stability of silylethynyl-substituted pentacene.<sup>11b</sup> The electrochemical HOMO-LUMO gap is 1.58 eV, which corresponds with the 790 nm (1.57 eV) HOMO-LUMO gap derived from the absorption spectrum (Figure 3). While solutions of **2** decompose slowly in the presence of air and light, the crystals can be stored in the dark for several months with no noticeable decomposition.

In stark contrast to hexacene **2**, the TTBS heptacene **4** was only sparingly soluble and marginally stable. Even under rigorously oxygen-free conditions, solutions of **4** decomposed within a day, and this decomposition accelerated when the solution was concentrated during attempted crystallization. The material was stable enough to obtain the UV-vis-NIR and proton NMR spectra, both of which support the structure **4**.

According to our empirical model for engineering the solid-state order of functionalized pentacene, crystalline derivatives are most easily obtained when the diameter of the solubilizing group is 35–50% of the length of the acene.<sup>11a</sup> Because the bulky TTBS group has a diameter slightly less (30%) than that size for heptacene, the even larger tris(trimethylsilyl)silyl (TTMSS) acetylene (diameter ~40% the width of heptacene) was used for the addition to heptacenequinone. Following addition of SnCl<sub>2</sub>, the reaction mixture turned a pale yellow-green color. Aqueous workup followed by



**Figure 2.** X-ray crystal structure of heptacene **5**.

chromatography on silica gel yielded a solution of heptacene **5**, which upon concentration and cooling yielded tiny, yellow-green flattened needlelike crystals (Figure 2). The crystals shattered if cooled below 150 K, but were stable at 200 K. Despite their size, diffraction was sufficiently sharp from one of the largest single needles (crystal size  $0.15 \times 0.02 \times 0.005$  mm, mass ca. 15 ng) for structure solution. The asymmetric unit contained one and two halves molecules of **5** with extensive disorder in the TMS groups. Nonetheless, the structure of heptacene **5** is unambiguous (Figure 2).<sup>16</sup> As with hexacene **2**, the aromatic core of heptacene **5** is essentially planar.

While solutions of **5** decompose in a few hours when exposed to air, the crystals are relatively stable, remaining unchanged for up to a week exposed to air and laboratory lighting. Heptacene **5** is very soluble, allowing characterization by <sup>1</sup>H and <sup>13</sup>C NMR, as well as cyclic voltammetry. The oxidation (0.470 V vs SCE) and reduction (−0.830 V vs SCE) potentials again show an electrochemical HOMO–LUMO gap that matches well with the gap extracted from the absorption edge of the optical spectrum (1.30 eV redox, 1.36 eV (912 nm) optical).

While there has been speculation that unsubstituted heptacene may possess an open-shell ground state, the sharp <sup>1</sup>H NMR signals obtained for **4** and **5** confirm that these functionalized heptacenes are closed-shell species. Analysis by EPR spectroscopy further supports the closed-shell nature of these compounds.

The absorption spectra of **2** and **5** are presented in Figure 3. Hexacene **2** has its longest-wavelength  $\lambda_{\text{max}}$  at 738 nm, corresponding to a 100-nm red-shift compared to that of a similarly substituted pentacene. Unlike **2**, heptacene **5** shows strong evidence for aggregate formation in its absorption spectrum. The longest-wavelength absorption in a good solvent ( $\text{CH}_2\text{Cl}_2$ ) is at  $\lambda_{\text{max}} = 852$  nm, with a pronounced shoulder at 825 nm. In a poor solvent (hexanes) this absorption is blue-shifted to  $\lambda_{\text{max}} = 835$ , with a second sharp peak at  $\lambda_{\text{max}} = 810$  nm. Nevertheless, the fusion of an additional aromatic ring leads to a further  $\sim 100$  nm red-shift in absorption compared to hexacene. A plot of the absorption edge of silylethynylated acenes anthracene–heptacene versus  $1/(\text{acene length})$  yields a y-intercept of 0.16 eV, suggesting a small but nonzero energy gap for the corresponding polymer, polyacene.

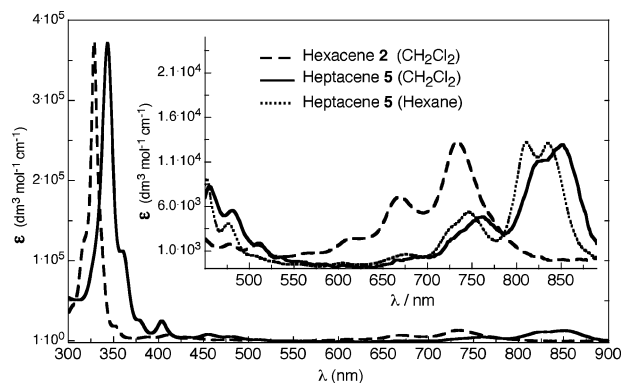


**Figure 3.** Electronic absorption spectra of **2** and **5** in dichloromethane. (Inset) Spectra of **2** and **5** in dichloromethane and of **5** in hexane.

**Acknowledgment.** We are grateful to the Office of Naval Research and the National Science Foundation (MRI No. 0319176) for support of this work. We thank Prof. M. R. Wasielewski (Northwestern University) for helpful discussion.

**Supporting Information Available:** Procedures for the preparation of **1–5**, characterization data, crystallographic CIF files for **2** and **5**, UV–vis–NIR spectra of silylethynyl-substituted anthracene–heptacene. This material is available free of charge via the Internet at <http://pubs.acs.org>.

## References

- Reese, C.; Roberts, M.; Ling, M.-M.; Bao, Z. *Mater. Today* **2004**, *20*.
- Campbell, R. B.; Robertson, J. M. *Acta Crystallogr.* **1962**, *15*, 289.
- (a) Clar, E. *Chem. Ber.* **1939**, *72B*, 2137. (b) Marschalk, C. *Bull. Soc. Chim.* **1939**, *6*, 1112. (c) Angliker, H.; Rommel, E.; Wirz, J. *Chem. Phys. Lett.* **1982**, *87*, 208.
- Bendikov, M.; Wudl, F.; Perepichka, D. F. *Chem. Rev.* **2004**, *104*, 4891.
- Bailey, W. J.; Liao, C.-W. *J. Am. Chem. Soc.* **1955**, *77*, 992.
- Clar, E. *Chem. Ber.* **1942**, *75*, 1283.
- Miller, G. P.; Briggs, J. *Org. Lett.* **2003**, *5*, 4203.
- Duong, H. M.; Bendikov, M.; Steiger, D.; Zhang, Q.; Sonmez, G.; Yamada, J.; Wudl, F. *Org. Lett.* **2003**, *5*, 4433 and references therein.
- (a) Schleyer, P. v. R.; Manoharan, M.; Jiao, H.; Stahl, F. *Org. Lett.* **2001**, *3*, 3643. (b) Wiberg, K. *J. Org. Chem.* **1997**, *62*, 5720. (c) Houk, K. N.; Lee, P. S.; Nendel, M. *J. Org. Chem.* **2001**, *66*, 5517 and references therein.
- Bendikov, M.; Duong, H. M.; Starkey, K.; Houk, K. N.; Carter, E. A.; Wudl, F. *J. Am. Chem. Soc.* **2004**, *126*, 7416.
- (a) Anthony, J. E.; Eaton, D. L.; Parkin, S. R. *Org. Lett.* **2002**, *4*, 15. (b) Maliakal, A.; Raghavachari, K.; Katz, H.; Chandross, E.; Siegrist, T. *Chem. Mater.* **2004**, *16*, 4980.
- For example, Morgenroth, F.; Berresheim, A. J.; Wagner, M.; Müllen, K. *Chem. Commun.* **1998**, 1138.
- Payne, M. M.; Odom, S. A.; Parkin, S. R.; Anthony, J. E. *Org. Lett.* **2004**, *6*, 3325.
- X-ray data for **2**; triclinic, space group  $P\bar{1}$ ;  $a = 8.5611(2)$  Å,  $b = 15.5772(4)$  Å,  $c = 18.1567(6)$  Å,  $\alpha = 75.3201(12)^\circ$ ,  $\beta = 81.3490(11)^\circ$ ,  $\gamma = 80.6678(12)^\circ$ ,  $V = 2296.09(11)$  Å<sup>3</sup>;  $Z = 1$ ;  $D_c = 1.118$  Mg·m<sup>−3</sup>;  $T = 90.0(2)$  K. Nonius KappaCCD diffractometer, graphite-monochromated sealed-tube Mo K $\alpha$  X-rays. Structure solved and refined using SHELX-97 (Sheldrick, G. M. Programs for crystal structure solution and refinement, Uni. Göttingen, Germany). Final  $R(F) = 5.47\%$ ,  $wR_2(F^2) = 13.92\%$  for 540 parameters and 10465 data.
- Sheraw, C. D.; Jackson, T. N.; Eaton, D. L.; Anthony, J. E. *Adv. Mater.* **2003**, *15*, 2009.
- X-ray data for **5**; triclinic, space group  $P\bar{1}$ ;  $a = 9.2305(4)$  Å,  $b = 24.6811(13)$  Å,  $c = 25.4062(12)$  Å,  $\alpha = 94.319(3)^\circ$ ,  $\beta = 95.069(3)^\circ$ ,  $\gamma = 91.020(3)^\circ$ ,  $V = 5747.3(5)$  Å<sup>3</sup>;  $Z = 1+2(1/2)$ ;  $D_c = 1.063$  Mg·m<sup>−3</sup>;  $T = 200(2)$  K. Bruker-Nonius  $\times 8$  Proteum diffractometer, multilayer-optic conditioned rotating-anode Cu K $\alpha$  X-rays. Structure solved and refined as in ref 14. Final  $R(F) = 8.06\%$ ,  $wR_2(F^2) = 13.92\%$  for 1142 parameters and 14577 data.

JA051798V